METABOLISM

Controlled-release mitochondrial protonophore (CRMP) reverses dyslipidemia and hepatic steatosis in dysmetabolic nonhuman primates

Leigh Goedeke[1], Liang Peng[1], Valle Montalvo-Romeral[1], Gina M. Butrico[1], Sylvie Dufour[1], Xian-Man Zhang[1], Rachel J. Perry[1,2], Gary W. Cline[1], Paul Kievit[3], Keefe Chng[4], Kitt Falk Petersen[1], Gerald I. Shulman[1,2]*

Nonalcoholic fatty liver disease (NAFLD) is estimated to affect up to one-third of the general population, and new therapies are urgently required. Our laboratory previously developed a controlled-release mitochondrial protonophore (CRMP) that is functionally liver-targeted and promotes oxidation of hepatic triglycerides. Although we previously demonstrated that CRMP safely reverses hypertriglyceridemia, fatty liver, hepatic inflammation, and fibrosis in diet-induced rodent models of obesity, there remains a critical need to assess its safety and efficacy in a model highly relevant to humans. Here, we evaluated the impact of longer-term CRMP treatment on hepatic mitochondrial oxidation and on the reversal of hypertriglyceridemia, NAFLD, and insulin resistance in high-fat, fructose-fed cynomolgus macaques (n = 6) and spontaneously obese dysmetabolic rhesus macaques (n = 12). Using positional isotopomer nuclear magnetic resonance tracer analysis (PINTA), we demonstrated that acute CRMP treatment (single dose, 5 mg/kg) increased rates of hepatic mitochondrial fat oxidation by 40%. Six weeks of CRMP treatment reduced hepatic triglycerides in both nonhuman primate models independently of changes in body weight, food intake, body temperature, or adverse reactions. CRMP treatment was also associated with a 20 to 30% reduction in fasting plasma triglycerides and low-density lipoprotein (LDL)–cholesterol in dysmetabolic nonhuman primates. Oral administration of CRMP reduced endogenous glucose production by 18%, attributable to a 20% reduction in hepatic acetyl–coenzyme A (CoA) content [as assessed by whole-body β-hydroxybutyrate (β-OHB) turnover] and pyruvate carboxylase flux. Collectively, these studies provide proof-of-concept data to support the development of liver-targeted mitochondrial uncouplers for the treatment of metabolic syndrome in humans.

INTRODUCTION

Caloric excess and a sedentary lifestyle have led to the global epidemic of obesity and metabolic syndrome (*1*), the hepatic consequence of which, nonalcoholic fatty liver disease (NAFLD), is estimated to affect up to one-third of the adult population in Western nations (*2*). This spectrum of liver disease is characterized by excessive cytoplasmic retention of triglycerides (*3*) and ranges from simple steatosis to nonalcoholic steatohepatitis (NASH), cirrhosis, and hepatocellular carcinoma (*4*). As rates of obesity continue to rise, NAFLD has become the most common cause of liver disease worldwide (*2*, *5*). In addition, NAFLD increases the risk for developing insulin resistance, type 2 diabetes (T2D), and cardiovascular disease (*6*–*8*).

Although the relationship between NAFLD and insulin resistance is complex and bidirectional (*9*), a substantial body of evidence in rodents and humans supports the role of ectopic lipid accumulation leading to impaired insulin action in the liver and skeletal muscle (*10*–*16*). In line with this, short-term caloric restriction reduces NAFLD and ectopic lipid accumulation and normalizes insulin sensitivity in rodent models of obesity and T2D (*17*). Lifestyle modifications remain the cornerstone of NAFLD and T2D management, with moderate weight reductions (<10%) causing a substantial decrease in hepatic fat content and improvements in hepatic insulin sensitivity in T2D patients (*18*). Despite this, in many individuals, these modifications cannot be implemented successfully or durably and new pharmacological agents are needed.

Liver-targeted mitochondrial uncoupling has recently gained attention as a potential therapeutic approach to increase hepatic fat oxidation and combat the life- and health-limiting consequences of NAFLD and T2D (*19*). Mitochondrial uncouplers [for example, 2,4-dinitrophenol (DNP)] shuttle protons across the inner mitochondrial membrane via a pathway that is independent of adenosine triphosphate (ATP) synthase, thereby uncoupling nutrient oxidation from ATP production (*20*). DNP has been known to increase metabolic rates since the late 1800s and was an effective and widely used weight loss drug in the 1930s (*21*–*24*). Unfortunately, chronic ingestion of DNP is associated with a number of unwanted side effects, including fatal hyperthermia and death, and was banned by the U.S. Food and Drug Administration (FDA) in 1938 (*25*). Nonetheless, given its ability to abrogate the development of NAFLD and hepatic insulin resistance in rats by promoting oxidation of hepatic triglycerides (*26*), we investigated whether DNP could be pharmacologically manipulated to improve its safety margin. In this regard, we recently developed a liver-targeted form of DNP (DNP methyl-ether), as well as a version of DNP with lower peak plasma concentrations and sustained release pharmacokinetics [controlled-release mitochondrial protonophore (CRMP)], and showed that these modified forms of DNP safely reverse hypertriglyceridemia, fatty liver, steatohepatitis, and liver fibrosis in rodent models of NAFLD, NASH, and T2D without inducing hyperthermia or associated hepatic and systemic toxicities (*27*–*29*). Although these studies suggested that mitochondrial protonophores may be a therapy for the major components of metabolic syndrome, their therapeutic utility for the treatment of NAFLD and T2D in a model highly relevant to

[1]Department of Internal Medicine, Yale School of Medicine, New Haven, CT 06510, USA. [2]Department of Cellular and Molecular Physiology, Yale School of Medicine, New Haven, CT 06510, USA. [3]Oregon National Primate Research Center, Oregon Health & Science University, Beaverton, OR 97006, USA. [4]Crown Bioscience Louisiana Inc., New Iberia, LA 70560, USA.
*Corresponding author. Email: gerald.shulman@yale.edu

humans remains unknown. For example, rodents do not typically develop spontaneous diabetes and many are resistant to the development of diet-induced obesity-mediated T2D, although they develop all symptoms of metabolic syndrome (*30*). Therefore, we aimed to determine the safety and efficacy of CRMP treatment over 6 weeks on the reversal of hypertriglyceridemia, NAFLD, and insulin resistance in diet-induced and spontaneous nonhuman primate models of metabolic syndrome that develop all clinical features of diabetes, including obesity, insulin resistance, dyslipidemia, and pancreatic pathology similar to humans. We hypothesized that CRMP treatment would reverse NAFLD and improve insulin sensitivity in obese nonhuman primates due to subtle sustained increases in rates of hepatic mitochondrial oxidation.

RESULTS

CRMP reverses NAFLD in high-fat, fructose-fed cynomolgus macaques

To determine whether CRMP could safely and effectively reverse NAFLD in a relevant nonhuman primate model of fatty liver and insulin resistance (*31*, *32*), we performed a pilot study in six high-fat, fructose-fed cynomolgus macaques. Briefly, cynomolgus macaques were fed a high-fat diet (HFD) along with fructose supplementation (in which 35% of calories were from fat) for 1 year. After a baseline characterization, we treated macaques with CRMP [0.8 mg/kg body weight twice daily (BID)] for 6 weeks, at which point we collected plasma and liver samples under general anesthesia. Clinical chemistry and body temperature were also assessed throughout the course of the study to ensure that animals remained in good health. A dose of 0.8 mg/kg (BID) was chosen on the basis of pharmacokinetic studies, which demonstrated that CRMP (0.8 mg/kg) treatment resulted in peak plasma DNP (the active moiety of CRMP) concentrations of 10 to 15 μM (fig. S1A). We previously established that this is well below the lower plasma concentration threshold for DNP toxicity in rodents (~400 μM) and slightly above the concentration needed to promote a sustained increase in hepatic mitochondrial fat oxidation (5 μM) (*27*, *28*). Six weeks of CRMP treatment was not associated with any appreciable differences in body temperature [a known on-target side effect of DNP (*33*)], blood pressure, heart rate, or food intake (fig. S1, B to E). Consistent with our rodent studies, chronic CRMP treatment significantly ($P = 0.05$) reduced endogenous glucose production (EGP) without altering body weight (Fig. 1, B to D, and fig. S1F). Although CRMP had no effect on fasting plasma triglycerides in this fructose-supplemented nonhuman primate model of metabolic syndrome (Fig. 1E), CRMP significantly increased plasma total cholesterol concentrations ($P = 0.02$), which could be attributed to increases in high-density lipoprotein cholesterol (HDL-C) (Fig. 1, F to H). Furthermore, there were no substantial differences observed in plasma alanine aminotransferase (ALT), aspartate aminotransferase (AST), blood urea nitrogen (BUN), or creatinine after chronic CRMP treatment (Fig. 1, I to L), indicating that 6 weeks of CRMP did not adversely affect liver or kidney function. Six weeks of CRMP treatment significantly reduced hepatic steatosis ($P = 0.04$) in high-fat, fructose-fed cynomolgus macaques, as evidenced by the 30% reduction in hepatic triglyceride content (Fig. 1M). Together, these data demonstrate that chronic CRMP treatment can safely and effectively reverse NAFLD in a diet-induced nonhuman primate model of fatty liver and insulin resistance.

CRMP is well tolerated in dysmetabolic rhesus macaques

We next determined the tolerability of CRMP in a larger spontaneous nonhuman primate model of NAFLD and T2D (*34*). To this end, two dysmetabolic rhesus macaques were administered daily escalating doses of CRMP (1, 5, 10, and 25 mg/kg) in banana mash (fig. S2A). No significant differences in body temperature were detected throughout the study, and both animals remained in good health (fig. S2B). We then examined the pharmacokinetic properties of CRMP after each dose. As shown in fig. S2 (C and D), oral dosing of CRMP (1 to 25 mg/kg) led to peak plasma concentrations of 8 to 140 μM DNP. No changes in plasma

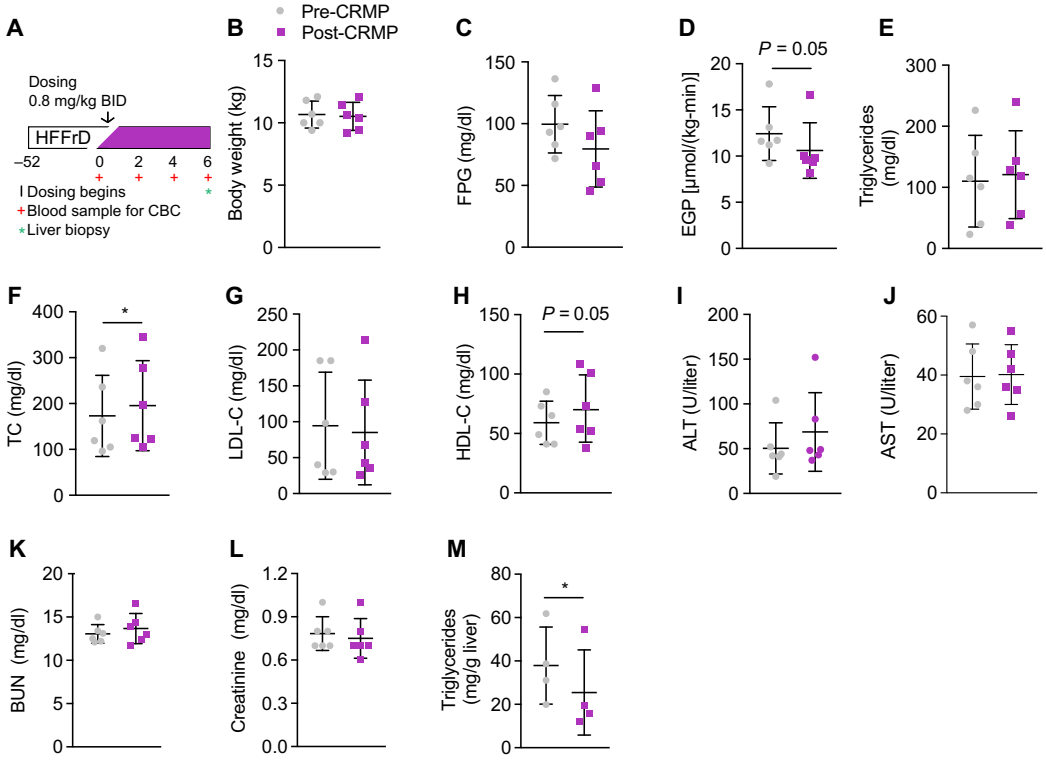

Fig. 1. CRMP reduces hepatic triglycerides in high-fat fructose-fed cynomolgus macaques. (**A**) Experimental outline of CRMP treatment in cynomolgus macaques. (**B** to **M**) Body weight (B), fasting plasma glucose (FPG) (C), EGP (D), plasma triglycerides (E), total cholesterol (TC) (F), LDL-C (G), HDL-C (H), ALT (I), AST (J), BUN (K), creatinine (L), and hepatic triglyceride content (M) in high-fat fructose-fed cynomolgus macaques before (pre-CRMP) and after CRMP (0.8 mg/kg BID) treatment for 6 weeks (post-CRMP). Data are means ± SD. In (B) to (L), $n = 6$ per treatment group. In (M), $n = 4$ per treatment group. *$P \leq 0.05$ by paired Student's t test (baseline versus treatment).

AST (aspartate aminotransferase), ALT (alanine aminotransferase), BUN, or creatinine were observed at any dose of CRMP tested (fig. S2, E to H), demonstrating that daily escalating doses of CRMP were well tolerated in rhesus macaques.

CRMP reduces plasma and hepatic lipids in dysmetabolic rhesus macaques

To assess the safety and efficacy of 6-week CRMP treatment on rates of hepatic mitochondrial oxidation and the reversal of hypertriglyceridemia, NAFLD, and insulin resistance in a highly relevant human model of metabolic syndrome, we performed a randomized control trial in spontaneously obese dysmetabolic rhesus macaques treated with CRMP [5 mg/(kg-day); $n = 12$] or vehicle control ($n = 6$) for 6 weeks (Fig. 2A), a dose that led to peak plasma DNP concentrations of 20 to 40 μM and was effective at acutely increasing rates of hepatic mitochondrial oxidation (citrate synthase flux, V_{CS}) (fig. S3, A to C, and Fig. 2B). As shown in Fig. 2 (C to E), CRMP treatment significantly reduced total fat mass ($P = 0.001$) independently of changes in body weight or lean mass. Nonhuman primates treated with CRMP also displayed a 30% reduction in plasma triglyceride concentrations (Fig. 2F) and a significant reduction in plasma total cholesterol ($P = 0.00002$), which could be attributed to a 30% reduction in very low-density lipoprotein cholesterol (VLDL-C) and low-density lipoprotein cholesterol (LDL-C) concentrations; plasma HDL-C concentrations

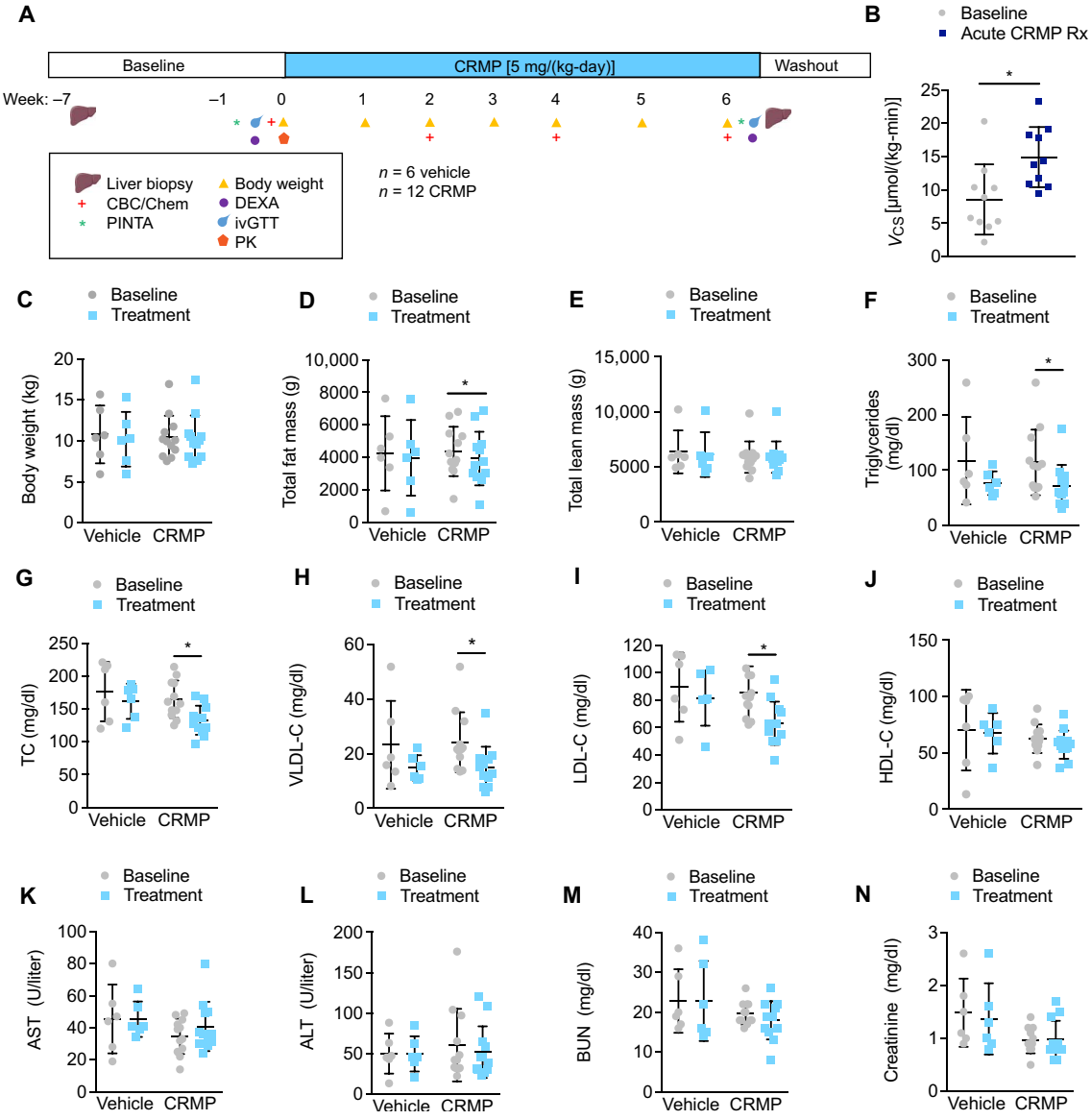

Fig. 2. CRMP treatment reduces plasma triglycerides, VLDL-C, and LDL-C in dysmetabolic rhesus macaques. (**A**) Experimental outline of the CRMP efficacy study in dysmetabolic rhesus macaques. (**B**) Citrate synthase flux (V_{CS}) in dysmetabolic rhesus macaques after acute treatment with CRMP (5 mg/kg; $n = 10$) or vehicle control ($n = 6$). *$P \leq 0.05$ by unpaired Student's t test. (**C** to **N**) Body weight (C), total fat mass (D), total lean mass (E), fasting plasma triglycerides (F), total cholesterol (TC) (G), VLDL-C (H), LDL-C (I), HDL-C (J), AST (K), ALT (L), BUN (M), and creatinine (N) in dysmetabolic rhesus macaques before (baseline) and after treatment with CRMP (5 mg/kg; $n = 12$) or vehicle control ($n = 6$) for 6 weeks (treatment). In (D), (G), and (I), *$P \leq 0.05$ by paired Student's t test (baseline versus treatment). In (F) and (H), *$P \leq 0.05$ by Wilcoxon matched-pairs signed rank test (baseline versus treatment). Data are means ± SD.

were unchanged (Fig. 2, G to J). No apparent toxicity was associated with 6-week CRMP treatment as shown by the clinical chemistries (ALT, AST, BUN, and creatinine) and blood counts, which remained within normal limits throughout the study (Fig. 2, K to N, and table S1). In addition, the hepatic glutathione (GSH)/oxidized glutathione (GSSG) ratio and protein carbonylation, markers of oxidative stress (*35*, *36*), were not significantly altered ($P > 0.05$) after 6 weeks of CRMP treatment (fig. S4, A and B).

CRMP reduces hepatic triglycerides in dysmetabolic rhesus macaques

Spontaneously obese dysmetabolic rhesus macaques often display hepatic histopathologic changes (fatty liver, inflammation, and fibrosis) that eventually progress to NAFLD/NASH (*34*). To evaluate the effect of CRMP treatment on hepatic steatosis, we measured the triglyceride content in liver biopsies from animals at baseline and after 6 weeks of CRMP treatment. Hepatic steatosis was not prominent in dysmetabolic rhesus macaques at baseline (Fig. 3A, mean triglyceride content ≤25 mg/g liver); nonetheless, CRMP did significantly reduce hepatic triglycerides by ~30% ($P = 0.05$, Fig. 3A). Given the key role of ectopic lipids in promoting hepatic insulin resistance (*26*, *37*), we next examined the effect of daily oral CRMP treatment on whole-body glucose metabolism and insulin resistance. Although CRMP tended to reduce fasting plasma insulin concentrations and homeostatic model assessment of insulin resistance (HOMA-IR), plasma glucose concentrations were unaltered (Fig. 3, B to D). Furthermore, no significant differences were observed in plasma glucose or insulin concentrations during an intravenous glucose tolerance test ($P > 0.05$; fig. S5, A to F).

CRMP increases rates of hepatic mitochondrial oxidation, reduces EGP, and improves hepatic insulin sensitivity in dysmetabolic rhesus macaques

We recently developed a noninvasive tracer method to model hepatic mitochondrial metabolism in vivo. This method, referred to as positional isotopomer nuclear magnetic resonance (NMR) tracer analysis (PINTA), assesses hepatic glucose production, pyruvate carboxylase flux (V_{PC}), and citrate synthase flux (V_{CS}) based on NMR and gas chromatography–mass spectrometry (GC-MS) analysis of plasma after an infusion of [3-^{13}C]lactate and [$^{2}H_7$]glucose (*38*). Using this approach, we examined V_{PC}/V_{CS} percent contributions of pyruvate to glucose and rates of gluconeogenesis in awake, overnight-fasted rhesus macaques before and after 6 weeks of treatment with CRMP [5 mg/(kg-day)]. In addition, we aimed to assess whether CRMP could produce chronic increases in hepatic mitochondrial oxidation rates (citrate synthase flux, V_{CS}). Using this PINTA approach, we found that acute CRMP treatment increased rates of V_{CS} by 40% (Fig. 2B). In contrast, there were no changes in V_{CS} 24 hours after the last dose of chronic (6 weeks) CRMP treatment, demonstrating that these effects were relatively short lived and not related to the 6-week treatment; relative rates of V_{PC}/V_{CS} and V_{PC}/V_{EGP} were also unchanged after chronic CRMP treatment (fig. S6, A to C). Consistent with this, DNP concentrations in chronically treated CRMP animals were not significantly different ($P > 0.05$) from vehicle controls (fig. S6D) and well below the concentration (<5 μM) needed to obtain increases in hepatic mitochondrial oxidation ($P = 0.006$, Fig. 2B). Despite this washout effect, these acute increases in V_{CS} (presumably occurring after each dose of CRMP over 6 weeks of treatment) were sufficient to increase hepatic insulin sensitivity and reduce EGP (Fig. 3, E and F). The reduction in rates of EGP could, in turn, be attributed to a 20% reduction in hepatic acetyl–coenzyme A (CoA) content [as reflected by reduced rates of whole-body β-hydroxybutyrate (β-OHB) turnover and plasma β-OHB concentrations (*39*)] and pyruvate carboxylase flux (Fig. 3, G and H, and fig. S6E). Linear regression analysis showed a strong relationship between percent reductions in EGP, V_{PC}, and whole-body β-OHB turnover (fig. S6, F to H).

PINTA measures hepatic mitochondrial fluxes with minimal pyruvate cycling in nonhuman primates

Studies from our laboratory have demonstrated that [3-^{13}C]lactate can be infused at a rate that provides sufficient label to measure hepatic mitochondrial fluxes without substantially altering hepatocellular mitochondrial metabolism (*38*, *40*, *41*). Specifically, the calculation of pyruvate carboxylase flux relative to citrate synthase flux (V_{PC}/V_{CS}) relies on the assumption that pyruvate cycling due to fluxes through pyruvate kinase (PK) or malic enzyme relative to V_{PC} is minimal and as such would need to be adjusted for accordingly. Although we have previously demonstrated that hepatic pyruvate cycling is relatively low in overnight-fasted rodents, healthy control human subjects, and insulin-resistant human subjects with NAFLD (*40*, *42*), this assumption has yet to be validated in nonhuman primates. We examined rates of hepatic mitochondrial oxidation and pyruvate cycling in a separate cohort

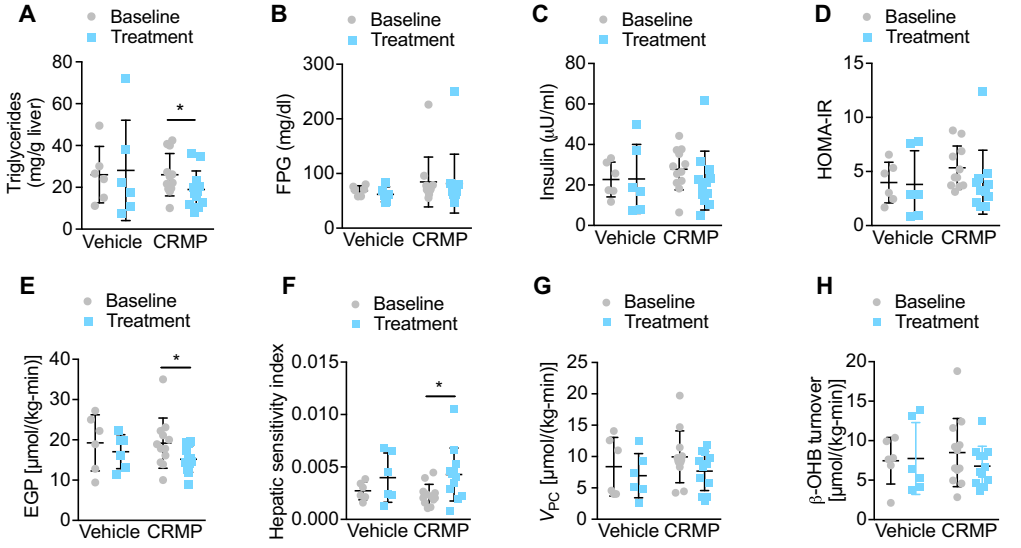

Fig. 3. CRMP treatment reduces hepatic triglycerides and EGP in dysmetabolic rhesus macaques. Hepatic triglycerides (**A**), fasting plasma glucose (FPG) (**B**), insulin (**C**), HOMA-IR (**D**), EGP (**E**), hepatic sensitivity index (**F**), pyruvate carboxylase flux (V_{PC}) (**G**), and β-OHB turnover (**H**) in dysmetabolic rhesus macaques before (baseline) and after treatment with CRMP (5 mg/kg; $n = 12$) or vehicle control ($n = 6$) for 6 weeks (treatment). *$P \leq 0.05$ by paired Student's t test (baseline versus treatment). In all panels, data are means ± SD.

of five dysmetabolic nonhuman primates following an infusion of [3-^{13}C]lactate and liver biopsy (Fig. 4A). We hypothesized that under fasting conditions, rates of pyruvate cycling (V_{PK}) would be minimal relative to rates of V_{PC} flux and would not affect our calculations of V_{PC}/V_{CS}. As shown in Fig. 4 (B and C), rates of V_{PC}/V_{CS} and V_{PC}/V_{EGP} were similar across the infusion study regardless of whether [^{13}C]glucose positional enrichments were measured in the liver or adjacent plasma samples [plasma 1 (P1) and plasma 2 (P2)]. Moreover, these fluxes correlated with V_{PC}/V_{CS} and V_{PC}/V_{EGP} rates identified in the cohort of dysmetabolic rhesus macaques used in our efficacy study (fig. S6, A and B). Furthermore, we observed no significant differences when we compared rates of V_{PC}/V_{CS} and V_{PC}/V_{EGP} calculated using PINTA or our previously validated ex vivo NMR method (Fig. 4, D and E), demonstrating the applicability of both methods across species. As expected after an overnight fast, rates of pyruvate dehydrogenase flux (V_{PDH}) relative to mitochondrial oxidation (V_{CS}) were minimal (<6%) (Fig. 4, F and G). Moreover, based on our previous calculations of V_{PC} (Fig. 3G), rates of hepatic V_{PK} flux were less than 40% that of V_{PC} flux (Fig. 4, H and I), consistent with previous human studies. Together, these data suggest that in overnight-fasted dysmetabolic rhesus macaques, pyruvate cycling is minimal and did not substantially affect our V_{PC} and V_{CS} flux estimates.

DISCUSSION

Over the past years, our understanding of the pathogenesis of NAFLD, insulin resistance, and T2D has improved, and with that, new pharmacological targets have emerged. Unfortunately, the complexity of insulin resistance and the presence of multiple feedback loops make it difficult to predict the consequences of a particular intervention, and as such, therapeutic interventions aimed at blocking biochemical pathways involved in glucose and lipid metabolism may prove difficult in practice (*19*). Promoting increased hepatic cellular energy expenditure through liver-targeted mitochondrial uncoupling may hold more promise. Multiple rodent studies support the use of small-molecule mitochondrial uncouplers for the treatment of metabolic syndrome despite their turbulent history in the clinic. Specifically, we have previously demonstrated that low-dose DNP treatment improves glucose tolerance, decreases plasma and liver triglyceride content, and reverses hepatic insulin resistance in an HFD-fed rat model of NAFLD (*26*), which has been replicated in HFD-fed mice (*43*, *44*). Our group has also shown that a liver-targeted methyl-ether derivative of DNP and a slow-release, functionally liver-targeted formulation of DNP (CRMP) can markedly increase the therapeutic window by 50- to 500-fold over DNP and that these drugs can safely reverse hepatic steatosis and hepatic inflammation and improve insulin sensitivity in rodent models of NAFLD/NASH, T2D, and lipodystrophy without any evidence of hyperthermia or systemic toxicity (*27*–*29*). Moreover, niclosamide ethanolamine, a salt form of the FDA-approved drug niclosamide, has also been shown to increase energy expenditure and lipid oxidation, and improve hepatic steatosis in diet-induced obese and *db/db* mice (*45*). Collectively, these studies demonstrate the beneficial effects of promoting subtle sustained increases in hepatic mitochondrial uncoupling to promote fat oxidation and support this approach for treating hepatic steatosis, NASH, insulin resistance, and T2D. However, to date, no studies have investigated the effects of hepatic mitochondrial uncoupling to treat metabolic syndrome in a model that closely resembles humans.

Here, in this pilot study, we examined the safety and efficacy of a functionally liver-targeted mitochondrial uncoupler (CRMP) on hypertriglyceridemia, hepatic steatosis, and insulin resistance in two old-world nonhuman primate models of metabolic syndrome: high-fat, fructose diet–induced obese cynomolgus macaques and spontaneously obese dysmetabolic rhesus macaques. Six weeks of CRMP treatment [0.8 mg/kg BID to 5 mg/(kg-day); peak plasma DNP concentrations of ~40 μM] did not cause any toxicity, inflammation, or other deleterious on-target side effects associated with systemic mitochondrial uncoupling (for example hyperthermia), demonstrating the feasibility of targeting DNP to the liver in nonhuman primates to improve its therapeutic index. Markers of liver function and oxidative stress also remained unchanged throughout the course of treatment in dysmetabolic rhesus macaques, suggesting that CRMP does not cause hepatic toxicity or promote oxidative stress in larger nonhuman primate models. Given that the 6-week no-observed-adverse-effect-level (NOAEL) of CRMP is 100 mg/kg in rodents (peak plasma concentrations of ~300 μM) (*28*), this was not surprising; however, the NOAEL of CRMP in nonhuman primates needs to be assessed in future studies.

Liver-targeted mitochondrial uncoupling has been shown to reduce hypertriglyceridemia and improve hepatic steatosis in rodents by increasing fat oxidation in the liver. With this study, we confirmed these findings in obese nonhuman primates. Specifically, CRMP treatment increased rates of

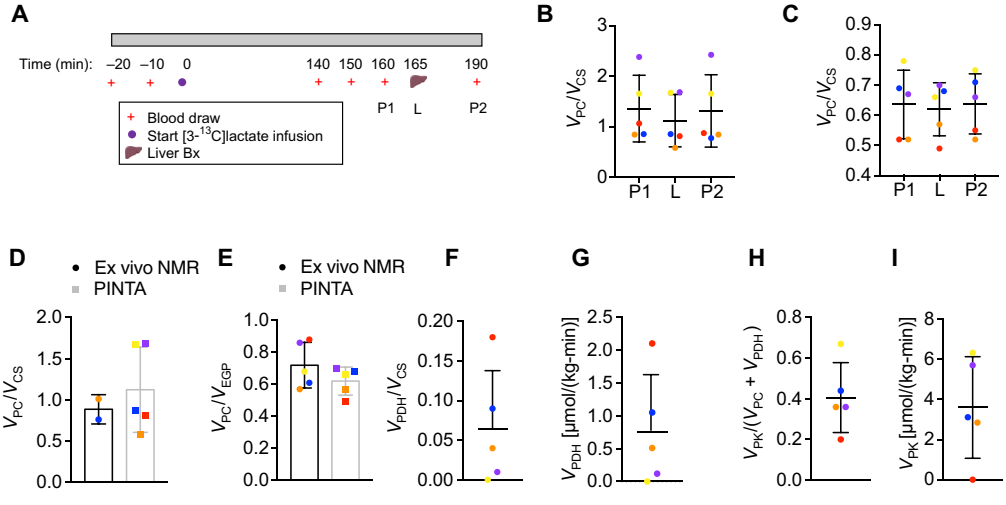

Fig. 4. Validation of PINTA to assess mitochondrial metabolism in nonhuman primates. (**A**) Experimental outline of [3-^{13}C]lactate infusion in dysmetabolic rhesus macaques (n = 5). (**B** and **C**) V_{PC}/V_{CS} (B) and V_{PC}/V_{EGP} in the plasma (P1 and P2) and livers of dysmetabolic rhesus macaques infused with [3-^{13}C]lactate [10 μmol/(kg-min)] for 190 min as assessed by PINTA. (**D** and **E**) V_{PC}/V_{CS} (D) and V_{PC}/V_{EGP} (E) in the livers of dysmetabolic rhesus macaques infused with [3-^{13}C]lactate [10 μmol/(kg-min)] for 190 min as assessed by ex vivo NMR (black bars) and PINTA (gray bars). (**F** to **I**) V_{PDH}/V_{CS} (F), V_{PDH} (G) $V_{PK}/V_{PC} + V_{PDH}$ (H), and V_{PK} (I) in the livers of dysmetabolic rhesus macaques infused with [3-^{13}C]lactate [10 μmol/(kg-min)] for 190 min. In (B) to (I), data are means ± SD. Each different color dot represents an individual animal.

Table 1. Characteristics of rhesus macaque cohorts.

Study	Animal ID	Sex	Age (years)	Body weight (kg)	Treatment
CRMP dose escalation	M632	F	16	12.1	–
	M254	F	26	8.3	–
CRMP efficacy	M956	F	9	13.74	Vehicle
	75P	F	16	10.38	Vehicle
	88J	F	19	5.92	Vehicle
	35S	F	16	10.68	Vehicle
	38F	F	22	8.34	Vehicle
	M767	M	13	15.65	Vehicle
	031	F	20	9.30	CRMP
	12K	F	19	10.20	CRMP
	M619	F	17	10.20	CRMP
	90J	F	19	8.10	CRMP
	98L	F	18	10.08	CRMP
	AC94	F	18	9.40	CRMP
	AH78	F	15	11.74	CRMP
	AL33	F	13	11.06	CRMP
	M254	F	27	7.52	CRMP
	M632	F	17	13.30	CRMP
	M741	M	14	16.93	CRMP
	68K	F	19	7.92	CRMP
Acute CRMP treatment	031	F	21	9.49	–
	M649	F	18	10.97	–
	90J	F	20	8.5	–
	M741	M	15	17.58	–
	98L	F	19	10.47	–
	AL33	F	15	11.43	–
	M632	F	18	13.74	–
	M956	F	10	15.09	–
	75P	F	18	9.86	–
	M787	M	14	15.98	–
PINTA validation	AH78	F	16	8.26	–
	15G	F	22	4.40	–
	33720	F	17	8.04	–
	68K	F	21	5.90	–
	37682	M	13	15.84	–

hepatic mitochondrial oxidation (citrate synthase flux, V_{CS}) assessed by PINTA, reduced plasma and hepatic triglycerides by 30%, and improved dyslipidemia. Previous studies have demonstrated that mitochondrial uncoupling will also activate 5′ AMP-activated protein kinase (AMPK) (*46*). Consequently, long-term CRMP treatment may reduce circulating LDL-C by activating AMPK, phosphorylating and inhibiting 3-Hydroxy-3-Methylglutaryl-CoA Reductase (HMGCR), and up-regulating hepatic expression of the SREBP2-responsive gene *LDLR* (*47*, *48*). Alternatively, CRMP may activate the SREBP2 pathway by reducing hepatic acetyl-CoA content, the precursor of cholesterol biosynthesis. Here, we showed that 6 weeks of CRMP treatment was associated with a 20% reduction in hepatic acetyl-CoA content [as reflected by β-OHB turnover (*39*)] in dysmetabolic rhesus macaques. Although the effect of CRMP treatment on the AMPK-Acetyl-CoA carboxylase (ACC) pathway and hepatic cholesterol synthesis remains to be determined, future studies are warranted to examine the therapeutic utility of CRMP to improve atherogenic dyslipidemia and treat cardiovascular disease.

In contrast with our previous rodent studies, 6 weeks of CRMP treatment did not affect fasting plasma glucose concentrations, insulin, or HOMA-IR, although it did decrease rates of EGP and increase the hepatic insulin sensitivity index. A recent publication demonstrated that spontaneously obese nonhuman primates have only mild hepatic alterations in insulin signaling. Despite being classified as "dysmetabolic," liver biopsies revealed that these macaques had no sign of excess hepatic fat, suggesting that this nonhuman primate model may not be ideal to examine lipid-induced insulin resistance (*49*). In our cohort, we observed minimal hepatic steatosis, with liver triglyceride content only reaching ~25 mg/g in liver tissue. In contrast, more pronounced hepatic steatosis was observed in high-fat, fructose-fed cynomolgus macaques. Moving forward, the effect of CRMP on whole-body insulin sensitivity should be assessed in diet-induced nonhuman primate models of obesity, which develop NAFLD/NASH, hepatic insulin resistance, and dysglycemia in a manner more similar to humans (*50*).

There is great interest in understanding the potential of therapies that modulate hepatic mitochondrial fat oxidation to reverse NAFLD. However, rates of hepatic mitochondrial fat oxidation have been difficult to assess in humans and results obtained using indirect approaches have been inconclusive. Moreover, using [$^{13}C_3$]propionate as a metabolic tracer, a recent study found that rates of hepatic mitochondrial oxidation and hepatic pyruvate cycling were two- to threefold greater in subjects with NAFLD compared to control subjects (*51*). In contrast, our laboratory has shown that rates of hepatic mitochondrial oxidation are not different between individuals with NAFLD and control subjects by using both in vivo ^{13}C magnetic resonance spectroscopy (MRS) (*38*)

Table 2. Characteristics of cynomolgus macaque cohort.

Study	Animal ID	Sex	Age (years)	Body weight (kg)
CRMP efficacy	A1	M	10	10.3
	A2	M	10	8.9
	A3	M	13	8.85
	A4	M	10	9.7
	A5	M	10	11.85
	A6	M	10	10.15

and PINTA (*38*, *42*) methodologies. We and others have previously attributed these discrepancies to possibly propionate-mediated disturbances in hepatic metabolism or pancreatic islet cell function (*40*, *52*). To further validate the PINTA methodology, we performed additional studies to directly assess rates of hepatic mitochondrial V_{PC} flux, pyruvate flux (V_{PK}), and V_{CS} flux in liver biopsies obtained in a subgroup of [3-^{13}C]lactate–infused rhesus macaques. Using this approach, we found that under fasting conditions, rates of V_{PK} were minimal relative to rates of V_{PC} flux, which is consistent with our previous in vivo ^{13}C MRS human study (*38*). Moreover, PINTA-determined ratios of V_{PC}/V_{CS} were comparable to V_{PC}/V_{CS} ratios assessed by our ex vivo NMR method, as well as to our previous ^{13}C MRS (*38*) and PINTA (*38*, *42*) human studies, providing additional in vivo validation of the PINTA methodology.

Several limitations of our study require further discussion. We have previously demonstrated that CRMP is liver-targeted by first-pass hepatic metabolism in rodent models of obesity, NAFLD/NASH, and T2D after oral delivery (*28*, *53*). However, we did not measure the tissue distribution of DNP (the active moiety of CRMP) in the current study. Given the on-target systemic toxicities of DNP (*25*), future studies using labeled CRMP and whole-body positron emission tomography (PET)–magnetic resonance imaging (MRI) or other methodologies should be considered in nonhuman primates to assess whether DNP accumulates in the brain or heart before moving to phase 1 clinical trials. Along these lines, long-term safety and efficacy studies with telemetry should also be conducted in nonhuman primates treated with CRMP. Another limitation is that the cohort of dysmetabolic rhesus macaques used in this study displayed little to no hepatic inflammation or fibrosis, which prevented us from assessing the effect of CRMP on NASH reversal. Previous studies have shown that CRMP can reduce inflammation and fibrosis in rodent models of NASH (*28*); therefore, studies examining the effect of CRMP to reverse hepatic fibrosis, inflammation, and stellate cell activation in nonhuman primates will be of great interest. Finally, due to the variability and small cohort of our obese nonhuman primate cohorts, we chose to conduct paired analyses when assessing the effect of CRMP on various metabolic parameters. Larger crossover studies in nonhuman primates comparing CRMP and vehicle-treated macaques are therefore warranted.

Despite these limitations, this pilot study demonstrated that CRMP safely and effectively improves dyslipidemia and hepatic steatosis in two nonhuman primate models of metabolic syndrome, providing proof-of-concept data for the development of liver-targeted mitochondrial uncoupling agents for the treatment of NAFLD/NASH and T2D and laying the groundwork for future nonhuman primate studies with liver-targeted mitochondrial uncouplers.

MATERIALS AND METHODS

Study design

The objectives of this study were to evaluate the safety and efficacy of CRMP treatment on hepatic mitochondrial oxidation and the reversal of hypertriglyceridemia, NAFLD, and insulin resistance in dysmetabolic nonhuman primates. In one set of experiments, male cynomolgus macaques were fed a HFD (TestDiet), along with fructose supplementation (in which 35% of calories were from fat) for 1 year. Animals were verified to be insulin-resistant and obese (body composition >30% fat) for at least 12 months. After a baseline characterization, macaques were given CRMP (0.8 mg/kg; BID) in approximately 1 teaspoon of banana mash for 6 weeks. In another set of experiments, spontaneously obese, dysmetabolic rhesus macaques were fed a low-fat, high–complex carbohydrate diet (Jumbo Macaque Diet) and randomized into two treatment groups: CRMP [5 mg/(kg-day)] or vehicle control (approximately 1 teaspoon of banana mash) for 6 weeks. The primary statistical outcome for this project was a reduction in hepatic triglyceride content assessed by liver biopsy before (baseline) and after 6 weeks of daily CRMP treatment. We also calculated that there would be sufficient power to assess the following secondary outcomes: hepatic citrate synthase flux, ketogenesis, and hepatic insulin sensitivity. Sample size was estimated to detect a difference in hepatic triglyceride content after 6 weeks of CRMP treatment and vehicle control based on the following assumptions: (i) type I error of 0.05, (ii) 90% power, (iii) a coefficient of variation of 40% for hepatic triglyceride content, and (iv) an effect size of 1.00 (that is, 27% of the expected mean of 3.66 before intervention). The sample size for individual experiments is indicated in the figure legends. Blinding was performed during data collection and analysis. For each experiment, the sample size reflects the number of independent biological replicates.

Inclusion and exclusion criteria

We included nonhuman primates that were 9 to 27 years of age at the prestudy (screening) evaluation, of male or female gender, and judged to be dysmetabolic on metabolic history and physical examination and specifically fulfilled at least four of seven metabolic parameters that have previously been shown to correlate with increased NAFLD/NASH in dysmetabolic nonhuman primates: total fat, >20%; waist circumference, >44 cm; fasting plasma glucose, >85 mg/dl; plasma triglycerides, >150 mg/dl; ALT, >40 U/liter (males) and >31 U/liter (females); AST, >37 U/liter (males) and >31 U/liter (females); and hepatorenal echo intensity (H/R) ratio, >1.4 (*34*). We excluded nonhuman primates that had a history of previous surgeries that might confound the results of the study or pose additional risk to the nonhuman primate by their participation in the study; had anemia, leukocytosis, thrombocytopenia, elevated liver and kidney values, and electrolyte disturbances; had history of pharmaceutical treatment within the past 3 months; or had a history of clinically significant endocrine, gastrointestinal, cardiovascular, hematological, hepatic, immunological, renal, respiratory, or genitourinary abnormalities or diseases. Although procedures were put in place to remove nonhuman primates from the study if an adverse event occurred [behavior deviated from normal (lethargy, discomfort, gastrointestinal symptoms, reduced food intake)], no macaques had to be removed and no outliers were excluded.

Rhesus macaque studies

Spontaneously obese, dysmetabolic rhesus macaques (*Macaca mulatta*; 9 to 27 years of age) of both sexes were singly housed at the Crown Bioscience Louisiana Center under a 12-hour light/dark cycle (6:00 p.m. to 6:00 a.m.) as previously described (*49*). Throughout the course of the study, macaques were given ad lib access to water and food (Jumbo Macaque Diet). In addition, each animal was given a variety of food treats (seasonal fruits and vegetables) three times a week. Unless otherwise specified, all studies were conducted in awake, chair-trained macaques. For the dose escalation study, two dysmetabolic rhesus macaques were enrolled and given CRMP (1, 5, 10, and 25 mg/kg) in banana mash every 3 days for a period of 16 days. Blood was taken at 0 (before dose), 2, 4, 8, 12, and 24 hours after each dose and immediately processed to plasma for subsequent analyses. For the efficacy study, 18 dysmetabolic rhesus macaques were enrolled and randomized into two treatment groups: vehicle ($n = 6$) and CRMP ($n = 12$). During the course of the study, animals received a voluntary, oral dose of CRMP [5 mg/(kg-day)] or vehicle control (banana mash). For the acute CRMP PINTA studies,

10 of the 18 nonhuman primates used in the efficacy study were enrolled. For the PINTA validation studies, five nonhuman primates were enrolled (two from the efficacy study plus an additional three dysmetabolic nonhuman primates).

The individual characteristics of the rhesus macaques used in each study are listed in Table 1.

All procedures were approved by the Institutional Animal Care and Use Committee at University of Louisiana at Lafayette, and guidelines set forth in the National Institutes of Health's *Guide for the Care and Use of Laboratory Animals* were followed. No animals were sacrificed or euthanized during the course of this study.

Cynomolgus macaque studies

Male cynomolgus macaques (*Macaca fascicularis*) were maintained on an HFD (TestDiet 5L0P, Purina) with fructose supplementation (35% of calories were from fat) for more than 1 year by the Obese Resource at Oregon National Primate Research Center (ONPRC) and singly housed. For the efficacy study, six obese, insulin-resistant cynomolgus macaques were enrolled and given CRMP (0.8 mg/kg; BID) in approximately 1 teaspoon of banana mash for 6 weeks. The individual characteristics of the cynomolgus macaques used in each study are listed in Table 2. All animal procedures were reviewed and approved by the Institutional Animal Care and Use Committee at the Oregon National Primate Research Center. No animals were sacrificed or euthanized during the course of this study.

Liver tissue biopsy

Liver biopsies were obtained from dysmetabolic rhesus macaques at baseline, after 6 weeks of treatment with CRMP (5 mg/kg; $n = 12$) or vehicle control ($n = 6$), and in a separate cohort of nonhuman primates used to validate PINTA for the assessment of hepatic mitochondrial metabolism. Briefly, overnight-fasted (16 hours) animals were sedated with ketamine (10 mg/kg) and anesthetized with propofol and isoflurane before the initiation of the surgical procedure. A small midline abdominal incision was made, and a piece of liver (about 1 g) was excised using the guillotine method. Liver samples were immediately flash-frozen in liquid nitrogen. Before, during, and after the surgery, vital signs were monitored and checked to ensure that they were within normal limits. All nonhuman primates were given at least 4 weeks of rest before any other procedures were conducted. Liver biopsies (~50 mg) were obtained from high-fat, fructose-fed cynomolgus macaques at baseline and after 6 weeks of treatment with CRMP (0.8 mg/kg BID) under isoflurane anesthesia per ONPRC standard operating procedures.

Body fat composition

Total body and fat trunk composition were assessed in anesthetized nonhuman primates by a dual-energy x-ray absorptiometry (DEXA) as previously described (*34*, *54*). Lunar Encore software (v13.6) was used to calculate fat, bone, and other mass for different regions of the body.

Glucose tolerance tests

Intravenous glucose tolerance tests were conducted in rhesus macaques as previously described (*55*). Briefly, after an overnight fast (16 hours), animals were sedated with an intramuscular dose of ketamine (10 mg/kg) and given a bolus of 50% dextrose (250 mg/kg) over 30 s through an intravenous cannula. Blood was then obtained through a separate intravenous cannula at 0 (before infusion), 3, 5, 7, 10, 15, 20, and 30 min after infusion and centrifuged immediately. Plasma glucose and insulin concentrations were measured as previously described (*55*).

CRMP PK and plasma DNP measurements

For the rhesus CRMP dose escalation study and on the first (day 1) and last day (day 42) of dosing during the rhesus efficacy study, blood samples were drawn from nonhuman primates at 0 (before dose), 2, 4, 8, 12, and 24 hours after CRMP administration to measure DNP concentrations. For the cynomolgus macaque CRMP PK study, unsedated blood samples were drawn at 0 (before dose 1), 1, 2, 3, 4, 5, 6, 7, 8, 9 (before dose 2), 10, 11, 24 (before dose 3), 25, 28, 30, 32, and 48 hours after CRMP administration. Blood samples were immediately centrifuged, and plasma was stored at −80°C. DNP concentrations were measured in the plasma by liquid chromatography–tandem mass spectrometry (LC-MS/MS) as previously described (*28*).

Clinical chemistry and observations

Blood pressure, heart rate, and core body temperature were collected continuously throughout the cynomolgus macaque study with implanted telemetry units (TSE Stellar Telemetry), and data were analyzed via Notocord software. Unsedated blood samples were collected biweekly in overnight-fasted cynomolgus macaques and immediately processed to plasma for assessment of glucose, triglycerides, total cholesterol, LDL-C, HDL-C, ALT, AST, BUN, and creatinine by COBAS as previously described (*28*). At days 1, 14, 28, and 42, overnight-fasted (16 hours) dysmetabolic rhesus macaques were chaired, weighed, and bled for specific metabolic parameters (complete blood count/clinical chemistry) as previously described (*49*). Hepatic sensitivity index was calculated using the following equation (Eq. 1):

$$\text{Hepatic sensitivity index} = \frac{1}{(\text{FPI} * \text{EGP})} \quad (1)$$

where

$$\text{FPI} = \text{fasting plasma insulin } (\mu\text{U/ml}) \quad (2)$$

and

$$\text{EGP} = \text{endogenous glucose production } \left(\frac{\text{mg}}{[\text{kg} - \text{min}]}\right) \quad (3)$$

Hepatic mitochondrial flux modeling

Mitochondrial fluxes were measured in overnight-fasted (16 hours) rhesus macaques during baseline and after 6 weeks of CRMP treatment [5 mg/(kg-day)] and in a separate cohort of macaques 1 hour after CRMP (5 mg/kg, oral) administration. Briefly, awake, chair-trained animals received a constant intravenous infusion of [3-^{13}C]lactate [10 μmol/(kg-min), 99% atom percent excess], [$^{2}H_7$]glucose [0.1 mg/(kg-min), 99% APE], and [$^{13}C_4$]β-OHB [0.01 mg/(kg-min)]. Blood was drawn at −20, −10, 140, 150, 160, 170, and 180 min and processed to plasma for subsequent analysis. Whole-body β-OHB turnover and glucose turnover (EGP) were calculated as previously described (*56*). Relative rates of V_{PC}/V_{CS} and V_{PC}/V_{EGP} were determined by PINTA as previously described (*38*) with minor modifications to correct for the possible contribution of [^{13}C]bicarbonate to label the tricarboxylic acid cycle metabolites (*57*).

In a separate set of experiments, lightly anesthetized, overnight-fasted (16 hours) rhesus macaques ($n = 5$) received a constant intravenous infusion of [3-^{13}C]lactate [10 μmol/(kg-min)] for 190 min. Blood was collected at −20, −10, 140, 150, 160, and 190 min and processed to

plasma for subsequent analysis; liver tissue (about 1 g) was obtained by laparoscopic surgery during the infusion and immediately snap-frozen at −80°C. Relative rates of hepatic and plasma V_{PC}/V_{CS} and V_{PC}/V_{EGP} were determined by PINTA and ex vivo NMR as previously described (*28*). Relative rates of $V_{PK}/V_{PC} + V_{PDH}$ and V_{PDH} were calculated as previously described (*40*, *42*). Pyruvate dehydrogenase flux (V_{PDH}) was calculated using the following equation (Eq. 4)

$$V_{PDH} = \frac{V_{PDH}}{V_{CS}} * V_{CS} \quad (4)$$

where V_{CS} is the mean V_{CS} from the baseline nonhuman primate studies calculated in fig. S6C. PK flux was calculated using the following equation (Eq. 5)

$$V_{PK} = \frac{V_{PK}}{V_{PC} + V_{PDH}} * (V_{PC} + V_{PDH}) \quad (5)$$

where V_{PC} is the mean V_{PC} from the baseline nonhuman primate studies calculated in Fig. 3G and V_{PDH} denotes pyruvate dehydrogenase flux calculated using Eq. 4.

Hepatic lipid measurements

Liver triglycerides were extracted by the method of Bligh and Dyer in overnight-fasted nonhuman primates and quantified using the Sekisui Triglyceride-SL Kit (Sekisui) as previously described (*10*).

Oxidative stress measurements

Protein carbonylation was determined in the livers (~50 mg) of dysmetabolic rhesus macaques at baseline and after 6 weeks of CRMP treatment using the Protein Carbonyl Colorimetric Assay Kit (Cayman Chemical) according to the manufacturer's instructions. The hepatic ratio of GSH/GSSG was determined by LC-MS/MS as previously described (*58*).

Statistical analysis

All data are expressed as mean ± SD. Statistical differences were measured using an unpaired or paired two-sided Student's *t* test when appropriate. Normality was checked using the Kolmogorov-Smirnov test. A nonparametric test (Wilcoxon matched-pairs signed rank test or Dunn's multiple comparison test) was used when data did not pass normality. A value of $P \leq 0.05$ was considered statistically significant. Data analysis was performed using GraphPad Prism software version 7 (GraphPad).

SUPPLEMENTARY MATERIALS

stm.sciencemag.org/cgi/content/full/11/512/eaay0284/DC1

Fig. S1. Safety and efficacy profile of CRMP-treated, high-fat, fructose-fed cynomolgus macaques.

Fig. S2. Oral CRMP dose escalation study in dysmetabolic rhesus macaques.

Fig. S3. Plasma DNP concentrations in dysmetabolic rhesus macaques.

Fig. S4. CRMP treatment does not alter oxidative stress in dysmetabolic rhesus macaques.

Fig. S5. CRMP treatment does not alter whole-body glucose tolerance in dysmetabolic rhesus macaques.

Fig. S6. Hepatic mitochondrial fluxes in dysmetabolic rhesus macaques treated with CRMP.

REFERENCES AND NOTES

1. B. A. Swinburn, G. Sacks, K. D. Hall, K. McPherson, D. T. Finegood, M. L. Moody, S. L. Gortmaker, The global obesity pandemic: Shaped by global drivers and local environments. *Lancet* **378**, 804–814 (2011).
2. Z. Younossi, Q. M. Anstee, M. Marietti, T. Hardy, L. Henry, M. Eslam, J. George, E. Bugianesi, Global burden of NAFLD and NASH: Trends, predictions, risk factors and prevention. *Nat. Rev. Gastroenterol. Hepatol.* **15**, 11–20 (2018).
3. Q. M. Anstee, H. L. Reeves, E. Kotsiliti, O. Govaere, M. Heikenwalder, From NASH to HCC: Current concepts and future challenges. *Nat. Rev. Gastroenterol. Hepatol.* **16**, 411–428 (2019).
4. A. D. Burt, C. Lackner, D. G. Tiniakos, Diagnosis and assessment of NAFLD: Definitions and histopathological classification. *Semin. Liver Dis.* **35**, 207–220 (2015).
5. Z. M. Younossi, A. B. Koenig, D. Abdelatif, Y. Fazel, L. Henry, M. Whymer, Global epidemiology of nonalcoholic fatty liver disease—Meta-analytic assessment of prevalence, incidence, and outcomes. *Hepatology* **64**, 73–84 (2016).
6. S. Ballestri, S. Zona, G. Targher, D. Romagnoli, E. Baldelli, F. Nascimbeni, A. Roverato, G. Guaraldi, A. Lonardo, Nonalcoholic fatty liver disease is associated with an almost twofold increased risk of incident type 2 diabetes and metabolic syndrome. Evidence from a systematic review and meta-analysis. *J. Gastroenterol. Hepatol.* **31**, 936–944 (2016).
7. V. T. Samuel, G. I. Shulman, Nonalcoholic fatty liver disease as a nexus of metabolic and hepatic diseases. *Cell Metab.* **27**, 22–41 (2018).
8. G. Targher, C. P. Day, E. Bonora, Risk of cardiovascular disease in patients with nonalcoholic fatty liver disease. *N. Engl. J. Med.* **363**, 1341–1350 (2010).
9. R. V. Farese Jr., R. Zechner, C. B. Newgard, T. C. Walther, The problem of establishing relationships between hepatic steatosis and hepatic insulin resistance. *Cell Metab.* **15**, 570–573 (2012).
10. M. C. Petersen, A. K. Madiraju, B. M. Gassaway, M. Marcel, A. R. Nasiri, G. Butrico, M. J. Marcucci, D. Zhang, A. Abulizi, X.-M. Zhang, W. Philbrick, S. R. Hubbard, M. J. Jurczak, V. T. Samuel, J. Rinehart, G. I. Shulman, Insulin receptor Thr^{1160} phosphorylation mediates lipid-induced hepatic insulin resistance. *J. Clin. Invest.* **126**, 4361–4371 (2016).
11. J. Szendroedi, T. Yoshimura, E. Phielix, C. Koliaki, M. Marcucci, D. Zhang, T. Jelenik, J. Müller, C. Herder, P. Nowotny, G. I. Shulman, M. Roden, Role of diacylglycerol activation of PKCθ in lipid-induced muscle insulin resistance in humans. *Proc. Natl. Acad. Sci. U.S.A.* **111**, 9597–9602 (2014).
12. Y. Li, T. J. Soos, X. Li, J. Wu, M. DeGennaro, X. Sun, D. R. Littman, M. J. Birnbaum, R. D. Polakiewicz, Protein kinase C θ inhibits insulin signaling by phosphorylating IRS1 at Ser^{1101}. *J. Biol. Chem.* **279**, 45304–45307 (2004).
13. K. W. Ter Horst, P. W. Gilijamse, R. I. Versteeg, M. T. Ackermans, A. J. Nederveen, S. E. la Fleur, J. A. Romijn, M. Nieuwdorp, D. Zhang, V. T. Samuel, D. F. Vatner, K. F. Petersen, G. I. Shulman, M. J. Serlie, Hepatic diacylglycerol-associated protein kinase Cε translocation links hepatic steatosis to hepatic insulin resistance in humans. *Cell Rep.* **19**, 1997–2004 (2017).
14. F. Magkos, X. Su, D. Bradley, E. Fabbrini, C. Conte, J. C. Eagon, J. E. Varela, E. M. Brunt, B. W. Patterson, S. Klein, Intrahepatic diacylglycerol content is associated with hepatic insulin resistance in obese subjects. *Gastroenterology* **142**, 1444–1446.e2 (2012).
15. J. K. Kim, O. Gavrilova, Y. Chen, M. L. Reitman, G. I. Shulman, Mechanism of insulin resistance in A-ZIP/F-1 fatless mice. *J. Biol. Chem.* **275**, 8456–8460 (2000).
16. K. F. Petersen, E. A. Oral, S. Dufour, D. Befroy, C. Ariyan, C. Yu, G. W. Cline, A. M. DePaoli, S. I. Taylor, P. Gorden, G. I. Shulman, Leptin reverses insulin resistance and hepatic steatosis in patients with severe lipodystrophy. *J. Clin. Invest.* **109**, 1345–1350 (2002).
17. R. J. Perry, L. Peng, G. W. Cline, Y. Wang, A. Rabin-Court, J. D. Song, D. Zhang, X.-M. Zhang, Y. Nozaki, S. Dufour, K. F. Petersen, G. I. Shulman, Mechanisms by which a very-low-calorie diet reverses hyperglycemia in a rat model of type 2 diabetes. *Cell Metab.* **27**, 210–217.e3 (2018).
18. K. F. Petersen, S. Dufour, D. Befroy, M. Lehrke, R. E. Hendler, G. I. Shulman, Reversal of nonalcoholic hepatic steatosis, hepatic insulin resistance, and hyperglycemia by moderate weight reduction in patients with type 2 diabetes. *Diabetes* **54**, 603–608 (2005).
19. L. Goedeke, R. J. Perry, G. I. Shulman, Emerging pharmacological targets for the treatment of nonalcoholic fatty liver disease, insulin resistance, and type 2 diabetes. *Annu. Rev. Pharmacol. Toxicol.* **59**, 65–87 (2019).
20. M. Jastroch, A. S. Divakaruni, S. Mookerjee, J. R. Treberg, M. D. Brand, Mitochondrial proton and electron leaks. *Essays Biochem.* **47**, 53–67 (2010).
21. M. L. Tainter, A. B. Stockton, W. C. Cutting, Use of dinitrophenol in obesity and related conditions. A progress report. *JAMA* **101**, 1472–1475 (1933).
22. M. L. Tainter, A. B. Stockton, Dinitrophenol in the treatment of obesity. Final report. *JAMA* **105**, 332–337 (1935).
23. W. C. Cutting, M. L. Tainter, Metabolic actions of dinitrophenol with the use of balanced and unbalanced diets. *JAMA* **101**, 2099–2102 (1933).
24. S. Simkins, Dinitrophenol and desiccated thyroid in the treatment of obesity: A comprehensive clinical and laboratory study. *JAMA* **108**, 2110–2117 (1937).
25. J. Grundlingh, P. I. Dargan, M. El-Zanfaly, D. M. Wood, 2,4-Dinitrophenol (DNP): A weight loss agent with significant acute toxicity and risk of death. *J. Med. Toxicol.* **7**, 205–212 (2011).

26. V. T. Samuel, Z.-X. Liu, X. Qu, B. D. Elder, S. Bilz, D. Befroy, A. J. Romanelli, G. I. Shulman, Mechanism of hepatic insulin resistance in non-alcoholic fatty liver disease. *J. Biol. Chem.* **279**, 32345–32353 (2004).
27. R. J. Perry, T. Kim, X.-M. Zhang, H.-Y. Lee, D. Pesta, V. B. Popov, D. Zhang, Y. Rahimi, M. J. Jurczak, G. W. Cline, D. A. Spiegel, G. I. Shulman, Reversal of hypertriglyceridemia, fatty liver disease, and insulin resistance by a liver-targeted mitochondrial uncoupler. *Cell Metab.* **18**, 740–748 (2013).
28. R. J. Perry, D. Zhang, X.-M. Zhang, J. L. Boyer, G. I. Shulman, Controlled-release mitochondrial protonophore reverses diabetes and steatohepatitis in rats. *Science* **347**, 1253–1256 (2015).
29. A. Abulizi, R. J. Perry, J. P. G. Camporez, M. J. Jurczak, K. F. Petersen, P. Aspichueta, G. I. Shulman, A controlled-release mitochondrial protonophore reverses hypertriglyceridemia, nonalcoholic steatohepatitis, and diabetes in lipodystrophic mice. *FASEB J.* **31**, 2916–2924 (2017).
30. J. D. Wagner, J. A. Cann, L. Zhang, H. J. Harwood, Diabetes and obesity research using nonhuman primates, in *Nonhuman Primates in Biomedical Research* (Academic Press, 2012), pp. 699–732.
31. M. A. Cydylo, A. T. Davis, K. Kavanagh, Fatty liver promotes fibrosis in macaques consuming high fructose. *Obesity* **25**, 290–293 (2017).
32. H. J. Harwood Jr., P. Listrani, J. D. Wagner, Nonhuman primates and other animal models in diabetes research. *J. Diabetes Sci. Technol.* **6**, 503–514 (2012).
33. R. A. Koch, R. C. Lee, M. L. Tainter, Dinitrophenol on liver function. *Cal. West. Med.* **43**, 337–339 (1935).
34. Y. Liu, H. Gu, H. Wang, B. Wang, X. Wang, G. Aoyagi, Y.-F. Xiao, K. Chng, X. Gao, J. Wang, E. Sho, Y.-P. Lin, Y. X. Wang, Hepatic steatosis and fibrosis in obese, dysmetabolic and diabetic nonhuman primates quantified by noninvasive echography. *J. Diabetes Metab.* **8**, 767 (2017).
35. I. Dalle-Donne, R. Rossi, D. Giustarini, A. Milzani, R. Colombo, Protein carbonyl groups as biomarkers of oxidative stress. *Clin. Chim. Acta* **329**, 23–38 (2003).
36. O. Zitka, S. Skalickova, J. Gumulec, M. Masarik, V. Adam, J. Hubalek, L. Trnkova, J. Kruseova, T. Eckschlager, R. Kizek, Redox status expressed as GSH:GSSG ratio as a marker for oxidative stress in paediatric tumour patients. *Oncol. Lett.* **4**, 1247–1253 (2012).
37. M. C. Petersen, G. I. Shulman, Roles of diacylglycerols and ceramides in hepatic insulin resistance. *Trends Pharmacol. Sci.* **38**, 649–665 (2017).
38. R. J. Perry, L. Peng, G. W. Cline, G. M. Butrico, Y. Wang, X.-M. Zhang, D. L. Rothman, K. F. Petersen, G. I. Shulman, Non-invasive assessment of hepatic mitochondrial metabolism by positional isotopomer NMR tracer analysis (PINTA). *Nat. Commun.* **8**, 798 (2017).
39. R. J. Perry, L. Peng, G. W. Cline, K. F. Petersen, G. I. Shulman, A non-invasive method to assess hepatic acetyl-CoA in vivo. *Cell Metab.* **25**, 749–756 (2017).
40. R. J. Perry, C. B. Borders, G. W. Cline, X.-M. Zhang, T. C. Alves, K. F. Petersen, D. L. Rothman, R. G. Kibbey, G. I. Shulman, Propionate increases hepatic pyruvate cycling and anaplerosis and alters mitochondrial metabolism. *J. Biol. Chem.* **291**, 12161–12170 (2016).
41. D. E. Befroy, R. J. Perry, N. Jain, S. Dufour, G. W. Cline, J. K. Trimmer, J. Brosnan, D. L. Rothman, K. F. Petersen, G. I. Shulman, Direct assessment of hepatic mitochondrial oxidative and anaplerotic fluxes in humans using dynamic ^{13}C magnetic resonance spectroscopy. *Nat. Med.* **20**, 98–102 (2014).
42. K. F. Petersen, D. E. Befroy, S. Dufour, D. L. Rothman, G. I. Shulman, Assessment of hepatic mitochondrial oxidation and pyruvate cycling in NAFLD by ^{13}C magnetic resonance spectroscopy. *Cell Metab.* **24**, 167–171 (2016).
43. M. Goldgof, C. Xiao, T. Chanturiya, W. Jou, O. Gavrilova, M. L. Reitman, The chemical uncoupler 2,4-dinitrophenol (DNP) protects against diet-induced obesity and improves energy homeostasis in mice at thermoneutrality. *J. Biol. Chem.* **289**, 19341–19350 (2014).
44. C. C. Caldeira da Silva, F. M. Cerqueira, L. F. Barbosa, M. H. Medeiros, A. J. Kowaltowski, Mild mitochondrial uncoupling in mice affects energy metabolism, redox balance and longevity. *Aging Cell* **7**, 552–560 (2008).
45. H. Tao, Y. Zhang, X. Zeng, G. I. Shulman, S. Jin, Niclosamide ethanolamine-induced mild mitochondrial uncoupling improves diabetic symptoms in mice. *Nat. Med.* **20**, 1263–1269 (2014).
46. G. Zhou, R. Myers, Y. Li, Y. Chen, X. Shen, J. Fenyk-Melody, M. Wu, J. Ventre, T. Doebber, N. Fujii, N. Musi, M. F. Hirshman, L. J. Goodyear, D. E. Moller, Role of AMP-activated protein kinase in mechanism of metformin action. *J. Clin. Invest.* **108**, 1167–1174 (2001).
47. M. S. Brown, J. L. Goldstein, The SREBP pathway: Regulation of cholesterol metabolism by proteolysis of a membrane-bound transcription factor. *Cell* **89**, 331–340 (1997).
48. P. R. Clarke, D. G. Hardie, Regulation of HMG-CoA reductase: Identification of the site phosphorylated by the AMP-activated protein kinase in vitro and in intact rat liver. *EMBO J.* **9**, 2439–2446 (1990).
49. J. Shang, S. F. Previs, S. Conarello, K. Chng, Y. Zhu, S. C. Souza, M. Staup, Y. Chen, D. Xie, E. Zycband, K. Schlessinger, V. P. Johnson, G. Arreaza, F. Liu, D. Levitan, L. Wang, M. van Heek, M. Erion, Y. Wang, D. E. Kelley, Phenotyping of adipose, liver, and skeletal muscle insulin resistance and response to pioglitazone in spontaneously obese rhesus macaques. *Am. J. Physiol. Endocrinol. Metab.* **312**, E235–E243 (2017).
50. P. J. Havel, P. Kievit, A. G. Comuzzie, A. A. Bremer, Use and importance of nonhuman primates in metabolic disease research: Current state of the field. *ILAR J.* **58**, 251–268 (2017).
51. N. E. Sunny, E. J. Parks, J. D. Browning, S. C. Burgess, Excessive hepatic mitochondrial TCA cycle and gluconeogenesis in humans with nonalcoholic fatty liver disease. *Cell Metab.* **14**, 804–810 (2011).
52. A. Tirosh, E. S. Calay, G. Tuncman, K. C. Claiborn, K. E. Inouye, K. Eguchi, M. Alcala, M. Rathaus, K. S. Hollander, I. Ron, R. Livne, Y. Heianza, L. Qi, I. Shai, R. Garg, G. S. Hotamisligil, The short-chain fatty acid propionate increases glucagon and FABP4 production, impairing insulin action in mice and humans. *Sci. Transl. Med.* **11**, eaav0120 (2019).
53. Y. Wang, A. R. Nasiri, W. E. Damsky, C. J. Perry, X. M. Zhang, A. Rabin-Court, M. N. Pollak, G. I. Shulman, R. J. Perry, Uncoupling hepatic oxidative phosphorylation reduces tumor growth in two murine models of colon cancer. *Cell Rep.* **24**, 47–55 (2018).
54. H. Gu, Y. Liu, S. Mei, B. Wang, G. Sun, X. Wang, Y. Xiao, M. Staup, F. M. Gregoire, K. Chng, Y. J. Wang, Left ventricular diastolic dysfunction in nonhuman primate model of dysmetabolism and diabetes. *BMC Cardiovasc. Disord.* **15**, 141 (2015).
55. M. Staup, G. Aoyagi, T. Bayless, Y. Wang, K. Chng, Characterization of metabolic status in nonhuman primates with the intravenous glucose tolerance test. *J. Vis. Exp.* , (2016).
56. L. Goedeke, J. Bates, D. F. Vatner, R. J. Perry, T. Wang, R. Ramirez, L. Li, M. W. Ellis, D. Zhang, K. E. Wong, C. Beysen, G. W. Cline, A. S. Ray, G. I. Shulman, Acetyl-CoA carboxylase inhibition reverses NAFLD and hepatic insulin resistance but promotes hypertriglyceridemia in rodents. *Hepatology* **68**, 2197–2211 (2018).
57. K. F. Petersen, S. Dufour, G. W. Cline, G. I. Shulman, Regulation of hepatic mitochondrial oxidation by glucose-alanine cycling during starvation in humans. *J. Clin. Invest.* 10.1172/JCI129913 (2019).
58. A. K. Madiraju, D. M. Erion, Y. Rahimi, X.-M. Zhang, D. T. Braddock, R. A. Albright, B. J. Prigaro, J. L. Wood, S. Bhanot, M. J. MacDonald, M. J. Jurczak, J.-P. Camporez, H.-Y. Lee, G. W. Cline, V. T. Samuel, R. G. Kibbey, G. I. Shulman, Metformin suppresses gluconeogenesis by inhibiting mitochondrial glycerophosphate dehydrogenase. *Nature* **510**, 542–546 (2014).

Acknowledgments: We thank K. Toussaint, J. Stack, M. Khan, I. Smolgovsky, G. Aoyagi, A. Gibson, M. Guy, R. Kennedy, and C. Thompson for their expert technical assistance. **Funding:** These studies were funded by grants from the U.S. Public Health Service (R01 DK113984, R01 DK119968, and P30 DK045735 to G.I.S.; K99 CA215315 to R.J.P.; and F32 DK114954 to L.G.), Gilead Sciences, and the U.S. NIH Office of the Director Grant (P51-OD-011092 for the operation of the ONPRC, support of the Obese Resource). **Author contributions:** The study was designed by L.G., K.F.P., P.K., K.C., and G.I.S. Data were collected and analyzed by L.G., L.P., V.M.-R., G.M.B., S.D., X.-M.Z., R.J.P., G.W.C., P.K., K.C., K.F.P., and G.I.S. The manuscript was written by L.G. and G.I.S. with contributions and approval from all authors. **Competing interests:** R.J.P. and G.I.S. are inventors on a Yale patent ("Novel 2,4-dinitrophenol formulations and methods using same") for liver-targeted mitochondrial uncoupling agents and controlled-release mitochondrial uncoupling agents for the treatment of NAFLD, NASH, T2D, and related metabolic disorders (WO 2015/031756 A1). G.I.S. serves on the advisory boards for Merck, Novo Nordisk, AstraZeneca, Gilead Sciences, and Janseen Research and Development, and he receives investigator-initiated support from AstraZeneca, Gilead Sciences, and Merck. K.F.P. receives investigator-initiated support from Merck. P.K. receives investigator-initiated support from Janssen Pharmaceuticals and Novo Nordisk. The other authors declare that they have no competing interests. **Data and materials availability:** All data associated with this study are present in the paper or in the Supplementary Materials.

Submitted 15 May 2019
Accepted 13 September 2019
Published 2 October 2019
10.1126/scitranslmed.aay0284

Citation: L. Goedeke, L. Peng, V. Montalvo-Romeral, G. M. Butrico, S. Dufour, X.-M. Zhang, R. J. Perry, G. W. Cline, P. Kievit, K. Chng, K. F. Petersen, G. I. Shulman, Controlled-release mitochondrial protonophore (CRMP) reverses dyslipidemia and hepatic steatosis in dysmetabolic nonhuman primates. *Sci. Transl. Med.* **11**, eaay0284 (2019).

Science Translational Medicine

Controlled-release mitochondrial protonophore (CRMP) reverses dyslipidemia and hepatic steatosis in dysmetabolic nonhuman primates

Leigh Goedeke, Liang Peng, Valle Montalvo-Romeral, Gina M. Butrico, Sylvie Dufour, Xian-Man Zhang, Rachel J. Perry, Gary W. Cline, Paul Kievit, Keefe Chng, Kitt Falk Petersen and Gerald I. Shulman

Sci Transl Med **11**, eaay0284.
DOI: 10.1126/scitranslmed.aay0284

Uncoupling mitochondria from liver disease

The mitochondrial uncoupler 2,4-dinitrophenol showed potential in treating nonalcoholic fatty liver disease (NAFLD) but was beset by toxicity issues. Here, Goedeke *et al.* show that a modified, liver-specific mitochondrial uncoupler, previously shown to be effective in rodent models of metabolic disease, improved metabolic symptoms in two diet-induced nonhuman primate models of NAFLD. Their controlled-release mitochondrial protonophore (CRMP) improved insulin resistance, dyslipidemia, and hepatic steatosis in nonhuman primates treated over the course of 6 weeks, without increases in oxidative stress, liver enzymes, or adverse events. This preclinical study supports further work to translate CRMP for the treatment of metabolic diseases in humans.